

Impurity-potential-induced gap at the Dirac point of topological insulators with in-plane magnetization

M.F. Islam,¹ Anna Pertsova,² and C.M. Canali¹

¹*Department of Physics and Electrical Engineering,
Linnaeus University, 391 82 Kalmar, Sweden*

²*Nordita, KTH Royal Institute of Technology and Stockholm University, Sweden*

(Dated: March 20, 2019)

The quantum anomalous Hall effect (QAHE), characterized by dissipationless quantized edge transport, relies crucially on a non-trivial topology of the electronic bulk bandstructure and a robust ferromagnetic order that breaks time-reversal symmetry. Magnetically-doped topological insulators (TIs) satisfy both these criteria, and are the most promising quantum materials for realizing the QAHE. Because the spin of the surface electrons aligns along the direction of magnetic-impurity exchange field, only magnetic TIs with an out-of-plane magnetization are thought to open a gap at the Dirac point (DP) of the surface states, resulting in the QAHE. Using a continuum model supported by atomistic tight-binding and first-principles calculations of transition-metal doped Bi_2Se_3 , we show that a surface-impurity potential generates an additional effective magnetic field which spin-polarizes the surface electrons along the direction perpendicular to the surface. The predicted gap-opening mechanism results from the interplay of this additional field and the in-plane magnetization that shifts the position of the DP away from the Γ point. This effect is similar to the one originating from the hexagonal warping correction of the bandstructure but is one order of magnitude stronger. Our calculations show that in a doped TI with in-plane magnetization the impurity-potential-induced gap at the DP is comparable to the one opened by an out-of-plane magnetization.

I. INTRODUCTION

TIs are a special class of quantum materials characterized by a non-trivial bulk band topology that results from band inversion at time-reversal invariant points of the Brillouin zone (BZ) due to strong spin-orbit coupling (SOC). TIs are insulating in the bulk but exhibit metallic behavior at their surfaces [1–3]. Since the discovery of TIs, several novel quantum phenomena have been predicted to emerge when long-range magnetic order is integrated into TIs. Among these are magnetic monopoles [4], giant magneto-optical effects [5], and the dissipationless inverse spin-Galvanic effect [6]. One of the most important applications of magnetic TIs is the realization of the QAHE, first predicted theoretically [7] and later confirmed experimentally in Cr- and V-doped $(\text{Bi}_2, \text{Sb}_2)\text{Te}_3$ magnetic TI [8–10]. Aside from three-dimensional (3D) TIs, the possibility of observing QAHE in two-dimensional (2D) buckled honeycomb atomic crystal layers with an in-plane magnetization has also been explored using microscopic models [11–13].

Theoretically, the topological surface states of a 3D TI near the DP are typically described by a phenomenological continuum 2D massless Dirac Hamiltonian, which results in a linear dispersion around the DP. In this simplified model, time reversal symmetry breaking terms such as the exchange field in a magnetic TI will open a gap at the DP only when the direction of magnetization is perpendicular to the plane of the surface states. In contrast, an in-plane magnetization shifts the position of the DP in the direction perpendicular to the magnetization, without opening any energy gap. On the other hand, for a realistic system, band structure calculations shows that non-linear corrections to the Dirac Hamilto-

nian become important away from the DP. For the TIs of the Bi_2Se_3 -family, Fu has shown [14] that the first of these non-linear corrections is a non-conventional cubic term, known as a hexagonal warping (HW) term. The HW term allows an in-plane magnetic field or magnetization to open a topological energy gap at the shifted DP of the surface states. Based on the Fu model, it has been predicted that QAHE can also be induced by in-plane magnetic order [15]. Theoretical studies of surface Mn-doped Bi_2Te_3 [16] and Bi_2Se_3 [17] TIs based on density functional theory (DFT) indeed confirm the possible appearance of an energy gap at the DP for an in-plane magnetization, in agreement with HW mechanism. More recent first-principles calculations [18] on Sb_2Te_3 covered with a ferromagnetic Fe monolayer also find similar small gaps for an in-plane magnetization. However, the surface-state energy gap for in-plane magnetization is typically much smaller (≈ 0.1 meV) than the gap for out-of-plane magnetization [16]. Based on these results, strong emphasis has been put on realizing magnetic TIs displaying a magnetic anisotropy that favors an out-of-plane magnetization [19].

Besides the coupling with the impurity-induced exchange field, the scattering of the surface electrons by the impurity potential can also affect the properties of the Dirac surface states by creating impurity resonance states. The theoretical approach [20, 21] used to address this problem is typically based on the usual purely 2D continuum phenomenological model of the surface states in the presence of an impurity potential. The strength of this scattering potential, which crucially determines the precise energy position and shape of the resonance states, is an unknown parameter. Note that this model is not able to capture the complexity of magnetic doping in 3D

TIs, whose effect in the density of states strongly depends on the TI material and type of impurity. Typically first-principles DFT calculations do not find evidence that such resonances occur right at the DP in case of magnetic doping [17, 18, 22]. Furthermore experiments [23–27] seem to indicate that these impurity resonances in the density of states reside tens of meV away from from the DP. Therefore these impurity resonances are typically not expected to affect the properties of the electronic structure right at the DP, although we cannot of course exclude that this might happen for some specific situations [28].

Some studies based on angular-resolved photoemission spectroscopy supported by first-principles calculations, carried out in non-TI material thin films, such as Ag(111) surface doped with Bi [29] or Si(111) surface doped with Ti [30], show the presence of a large spin splitting of the surface electrons in the direction normal to the surface, which cannot be explained by the ordinary Rashba effect and is attributed to the impurity potential and SOC. Essentially, the idea emerging in these studies is that the Bi-ion doping in Bi/Ag(111) and the adsorbed Ti monolayer in Ti/Si(111) creates a strong *in-plane* gradient of the crystal potential in the surface layer. This gradient, in analogy with the ordinary Rashba effect, gives rise to an effective magnetic field, which is directed *out-of-plane*. In magnetic TIs, where magnetic order is induced by doping, the impurity potential may as well result in a non-zero spin-polarization of the surface electrons normal to the surface. Such a “magnetic” influence of the impurity potential on the spin properties of the Dirac surface states has not been considered before. As we show below, when an in-plane magnetization is present, this additional spin polarization can contribute to opening a gap at the DP in a way similar to the Fu’s HW mechanism. However, in contrast to the very small HW-induced gap, the impurity-potential-induced gap is of the same size of the gap generated by an out-of-plane magnetization. This result implies that the conditions for realizing the QAHE might be less stringent than what originally anticipated. Careful manipulation of the doping potential-gradient might also allow a novel way to enhancing the gap at the DP, leading to the realization of the QAHE at higher temperatures.

II. CONTINUUM MODEL

The Hamiltonian of the 2D surface states in the presence of magnetic impurities with arbitrary magnetiza-

tion, \mathbf{M} , is given by

$$\begin{aligned} \mathcal{H}_{\mathcal{D}}(k) &= E_0(k) + v_f(k_x\sigma_y - k_y\sigma_x) + \lambda(k_+^3 + k_-^3)\sigma_z \\ &\quad + \frac{J}{2}\mathbf{M} \cdot \boldsymbol{\sigma} + \mathbf{B}^i(\mathbf{k}) \cdot \boldsymbol{\sigma} \\ &= E_0(k) - (v_f k_y - \frac{J}{2}M_x - B_x^i(\mathbf{k}))\sigma_x \\ &\quad + (v_f k_x + \frac{J}{2}M_y + B_y^i(\mathbf{k}))\sigma_y \\ &\quad + (\frac{J}{2}M_z + \lambda(k_+^3 + k_-^3) + B_z^i(\mathbf{k}))\sigma_z, \end{aligned} \quad (1)$$

where $E_0(k) = \frac{\hbar^2 k^2}{2m^*}$. The second term in Eq. 1 is the usual 2D Dirac Hamiltonian, giving a linear \mathbf{k} dependence around the DP located at $\mathbf{k} = \mathbf{0}$. The third term is the HW term, i.e. a cubic correction to the linear Dirac Hamiltonian [14] where $k_{\pm} = k_x \pm ik_y$. The fourth term is the exchange coupling between the surface electrons specified by spin operator $\boldsymbol{\sigma}$ and the impurity magnetic moment \mathbf{M} , with J being the exchange energy. The last term corresponds to the exchange interaction between the surface electrons and an effective magnetic field \mathbf{B}^i coming from the potential gradient created by the impurity. It can be described phenomenologically as [30]

$$\mathbf{B}^i(\mathbf{k}) \approx \frac{\hbar^2 N}{mc^2 \Omega} \int_{\text{cell}} d\mathbf{r} \frac{1}{r} \frac{dV(\mathbf{r})}{dr} u_{n\mathbf{k}}^*(\mathbf{r}) \mathbf{L} u_{n\mathbf{k}}(\mathbf{r}), \quad (2)$$

where, $V(\mathbf{r})$ is the electronic potential, \mathbf{L} is the angular momentum operator, $u_{n\mathbf{k}}(\mathbf{r})$ are Bloch functions and Ω is the volume of the primitive unit cell containing N atoms. The effective magnetic field \mathbf{B}^i is proportional to the average value of the angular momentum \mathbf{L} weighted by the potential gradient. The field \mathbf{B}^i incorporates the symmetry properties of the lattice via the Bloch functions, which is then reflected in the symmetry properties of the band structure and spin-polarization of the surface states, as clearly evinced in both experimental studies [29, 30]. Eq. 2 also shows that the \mathbf{B}^i field vanishes at time-reversal invariant \mathbf{k} -vectors, such as the Γ point.

Defining $\mathbf{M} = (M_{\parallel} \cos \beta, M_{\parallel} \sin \beta, M_z)$, $\mathbf{B}^i = (B_{\parallel}^i \cos \gamma, B_{\parallel}^i \sin \gamma, B_z^i)$ and surface wavevector $\mathbf{k} = (k \cos \theta, k \sin \theta)$, where M_{\parallel} , B_{\parallel} are the projections of \mathbf{M} and \mathbf{B}^i parallel to the surface (x - y plane), respectively, and the angles are defined relative to the x -axis, the spectrum of the system can be obtained by diagonalizing the Hamiltonian in Eq. 1

$$\begin{aligned} E(\mathbf{k}) &= E_0 \pm \epsilon(\mathbf{k}) \\ \epsilon(\mathbf{k}) &= \sqrt{[v_f^2 k^2 + B_{\parallel}^2(\mathbf{k}) + \frac{J^2}{4} M_{\parallel}^2 + J B_{\parallel}^i(\mathbf{k}) M_{\parallel} \cos(\beta - \gamma) \\ &\quad + 2v_f B_{\parallel}^i(\mathbf{k}) k \sin(\gamma - \theta) + J v_f M_{\parallel} k \sin(\beta - \theta) \\ &\quad + (B_z^i(\mathbf{k}) + \frac{J}{2} M_z + \lambda k^3 \cos 3\theta)^2]}. \end{aligned} \quad (3)$$

It is evident from Eq. 1 that the out-of-plane component of \mathbf{M} breaks the spin degeneracy at the DP by aligning

spins of the surface electron along the normal, and consequently, a gap opens up at the DP, as evinced by Eq. 3. On the other hand, the in-plane components of magnetization, \mathbf{M} , only shifts the DP of a TI from the Γ -point to a point along the direction perpendicular to M_{\parallel} , but does not contribute to the gap opening at the DP. The amount of the shift of the DP depends on the strength of the in-plane components of \mathbf{M} . This shift can be also influenced by the in-plane component of \mathbf{B}^i .

The HW term in Eq. 1 results in a non-zero out-of-plane component of the surface spins given by [14] $S_z(\mathbf{k}) = \cos(3\theta)/\sqrt{\cos^2(3\theta) + 1/(ka)^4}$, where $a = \sqrt{\lambda/v_f}$. Note that $S_z(\mathbf{k})$ vanishes at the Γ point and its value away from the Γ point is controlled by the strength of the HW term λ relative to the Fermi velocity v_f . It follows that the combined interplay of the in-plane magnetization (which shifts the DP away from the Γ point) and the HW-induced $S_z(k)$ can open up a gap at the shifted DP. This was already pointed out by Fu [14]. The effective magnetic field B_z^i , caused by the impurity potential, gives rise to a similar mechanism: it causes an additional out-of-plane spin polarization at \mathbf{k} away from the DP. This impurity-potential-induced spin-polarization can therefore contribute to the energy gap at a DP which has been shifted by an in-plane polarization. As we will see below, the effect of B_z^i on the energy gap is typically larger than the one caused by the HW term.

III. RESULTS BASED ON ATOMISTIC TB METHOD

To support the theoretical predictions based on the continuum model of Eq. 1, we used a microscopic tight-binding (TB) model with parameters fitted to DFT calculations obtained with Wien2k [31]. The TB model for pristine Bi_2Se_3 includes s and p orbitals and Slater-Koster hopping elements between atoms in the same atomic layer and between atoms in first and second nearest-neighbor layers. SOC is incorporated in the intra-atomic matrix elements. Since the TB parameters are fitted to DFT calculations, the TB model contains inherently higher-order corrections to the linear dispersion of the surface states, such as the HW term. The TB model is particularly useful for discerning small energy gaps at DP, which is problematic in DFT.

For surface calculations with impurity doping, we consider a slab consisting of six quintuple layers (QLs) and a 3×3 surface supercell [32]. An impurity substitutes a Bi atom on the top surface and is described by a local magnetic moment and an on-site potential [22]. The impurity magnetic moment is treated as a classical spin, modeled by a local exchange field \mathbf{M} coupled to the electron spin at the impurity site. For the non-magnetic part of the impurity potential, we consider two cases: (i) a point-like impurity potential U , which acts as a uniform shift to the on-site energy of the impurity atom; (ii) a realistic impu-

rity potential, which includes the on-site potential U and a modification of the hopping parameters between the impurity and its neighbors (in our calculations, all hopping parameters around the impurity are modified by equal amounts). The impurity potential U is known to introduce localized impurity states that can affect electronic states in the vicinity of the DP [21]. Here, however, we focus on modifications exactly at the DP. For the value of the impurity potential used in this work, the impurity resonant states are located in the valence band (approximately 400 meV below the DP of the bottom surface states for $U=4$ eV).

The results of TB bandstructure calculations for a particular choice of parameters are shown in Fig. 1 for a point-like (a,b) and a realistic (c,d) impurity, plus an in-plane magnetic moment. \mathbf{M} is chosen to point in the Γ - K direction of the surface BZ. We specifically choose this direction since the effect of the HW term is identically zero for exchange fields in the Γ - K direction [14]. The bands are plotted in the perpendicular (Γ - M) direction. As one can see from Fig. 1(a), the impurity doping affects the Dirac states of the top surface (where impurity is located) in several important ways. There is an expected shift of the top surface DP in momentum space in the direction perpendicular to \mathbf{M} . In addition, the DP shifts in energy due to the on-site potential U . Importantly, in the absence of the HW term and for a point-like impurity, the top surface DP remains gapless [see Fig. 1(b)]. Figure 1(b) also shows an energy gap of order of 1 meV resulting from an avoided level crossing between the top and bottom Dirac states which are still coupled in a six QLs slab. The Dirac cone of the bottom surface is unaffected by the impurity.

In contrast to the case of a point-like impurity, a more realistic impurity potential with modified hopping matrix elements will generate an in-plane electric field giving rise to an effective *out-of-plane* magnetic field that can gap the DP. This is confirmed by our TB calculations presented in Fig. 1(c) and (d): the zoom-in of the bandstructure around the shifted top surface DP reveals an energy gap, $\Delta_{\text{DP}} \approx 1$ meV. Since the HW term is zero for \mathbf{M} pointing along Γ - K , this gap can be attributed solely to the effective exchange field created by the impurity potential. This is precisely the effect expected based on continuum-model arguments. Further analysis of the bands in 3D momentum space for a few choices of parameters (hoppings reduced/increased by 20% and 40%), confirmed that the DP is gapped and is located along Γ - M . There is an additional shift of DP along Γ - M , relative to the shift due to the impurity magnetic moment. This suggests that for this specific simplified model of a realistic impurity potential (and within the momentum resolution of 0.001\AA^{-1}), the in-plane projection of the impurity-potential-induced magnetization is finite and is pointing perpendicular to Γ - M .

In order to compare the size of the impurity-potential-induced gap with the size of the gap due the HW term, we have carried out additional calculations (not shown here).

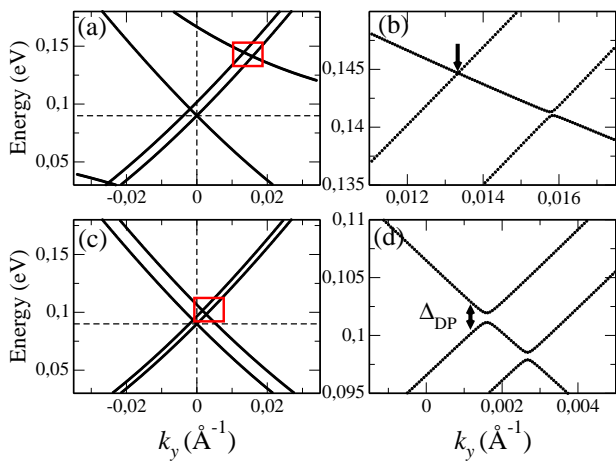


FIG. 1. TB bandstructure calculations for a six QL Bi_2Se_3 thin film with a magnetic impurity on the top surface. (a,b) Point-like impurity with an in-plane magnetic moment \mathbf{M} ($|\mathbf{M}| = 2$ eV) and on-site potential $U = 4$ eV. (c,d) Realistic impurity with modified hopping parameters between the impurity site and its neighbor atoms (hopping matrix elements are reduced by 20%). The values of \mathbf{M} and U are the same as in panels (a,b). Panels (b) and (d) show small regions of the bandstructures marked by red squares in panels (a) and (c) respectively. Dashed lines mark the position of the bottom surface DP. Vertical arrow in (b) shows the top-surface DP. Impurity-potential-induced gap, $\Delta_{\text{DP}} \approx 1$ meV, is indicated in (d).

For a point-like impurity with magnetic moment along Γ - M , the resulting gap is solely due to the HW term and is an order of magnitude smaller than the impurity-potential-induced gap, $\Delta_{\text{HW}} = 0.07 \approx 0.1$ meV. For the case where both the HW term and the impurity-induced magnetic field are present, namely for a realistic impurity with magnetic moment along Γ - M , the gap at DP remains essentially the same as that shown in Fig. 1(d), $\Delta_{\text{DP}} \approx 1$ meV. This further confirms that the HW gap is much smaller than the impurity-potential-induced gap.

IV. DFT RESULTS

To investigate the relative strength of the HW effect and the impurity-induced field for a realistic system, we have performed DFT calculations for Mn- and Fe-doped Bi_2Se_3 surfaces to calculate the surface spin-polarization induced by these two effects. The DFT calculations are carried out using the all-electron LAPW method with PBE exchange correlation functional [33] as implemented in the WIEN2k code[34]. We have constructed a 2×2 surface supercell containing six QLs. The impurity is added by substituting a Bi atom only from the topmost Bi layer, as shown in Fig. 2a. The doped surface has been relaxed. To obtain the easy axis, we have calculated the single-ion anisotropy (SIA) by performing two sets of calculations self-consistently, including SOC: one with

the out-of-plane magnetization and the second one with the in-plane magnetization along $\langle 111 \rangle$ (Γ -K path in the BZ), as shown in Fig 2. This particular choice of in-plane magnetization is important for computational purposes, as it preserves one mirror symmetry that considerably reduces the size of the problem, and allows us to calculate SIA self-consistently.

We find that for Mn, the SIA is small (0.08 meV) with an *out-of-plane* easy axis. For Fe, the SIA is considerably larger (1.5 meV) with an *in-plane* easy axis. According to Eq. 1, the DP remains at the Γ -point for Mn-doping. But for Fe-doping, it shifts away from the Γ -point along M- Γ -M path (normal to the magnetization direction), which is confirmed by the TB calculations discussed above. Since the HW- and impurity-induced field are effective only for an in-plane magnetization, here we consider only Fe-doped Bi_2Se_3 . As mentioned in the discussion of continuum model, the gap at the shifted DP results from the combined effect of HW and B_z^i . To disentangle these two contributions and study their relative strengths, we proceed as follows. We note from Eq. 2 that \mathbf{B}^i has the same dependence as the expectation value of the orbital momentum operator, \mathbf{L} . It is convenient to identify the HW term in Eq. 1 as an internal magnetic field, $B_{\text{HW}}(\mathbf{k}) = \lambda(\mathbf{k}_+^3 + \mathbf{k}_-^3)$, pointing along the z direction. Since the HW term describes a cubic SOC at the surface of rhombohedral crystal systems, the field $B_{\text{HW}}(\mathbf{k}) \sim L_z(\mathbf{k})$. Therefore, the atomic orbital moments, $\mathbf{L}^{\text{atom}}(\mathbf{k})$, of the surface atoms can provide important insight about the relative strength of these two contributions and their \mathbf{k} -dependence. The HW term affects the Dirac surface states of both the top and the bottom surface of the slab in the same way. Therefore, we expect that both $L_z^{\text{atom}}(\mathbf{k})$ and $S_z^{\text{atom}}(\mathbf{k})$ will be essentially the same for atoms at or close to the top and the bottom surface. On the other hand, since the magnetic impurity is added only at the top surface of the slab, the induced field B_z^i is expected to affect only the Dirac surface states of the top surface, which will be then reflected in a strong dependence of the local orbital and spin components of the surface atoms.

Since Fe doping causes a shift the DP along M- Γ -M' path, we have calculated the expectation values of the \mathbf{L} and the \mathbf{S} operators along this path. As discussed above, the impurity-induced field influences only the atoms at the top surface and is expected to be strong for atoms that are nearest to the Fe atom. Therefore, we have calculated $\langle \mathbf{L} \rangle$ and $\langle \mathbf{S} \rangle$ for the Bi atom located in the same plane of the Fe impurity (see Fig 2a). In order to distinguish this effect from the HW effect, we have selected a Se atom from the bottom layer where only the HW effect is expected to play a significant role. The results are plotted in Fig 2. We note from Fig 2b that the k -dependence of the in-plane components of $\langle L_{x,y} \rangle$ is similar and comparable in magnitude both at the top and the bottom surfaces, except that the sign is reversed, which is a reflection of the fact that helicity is opposite at the two surfaces. On the other hand, it is evident that

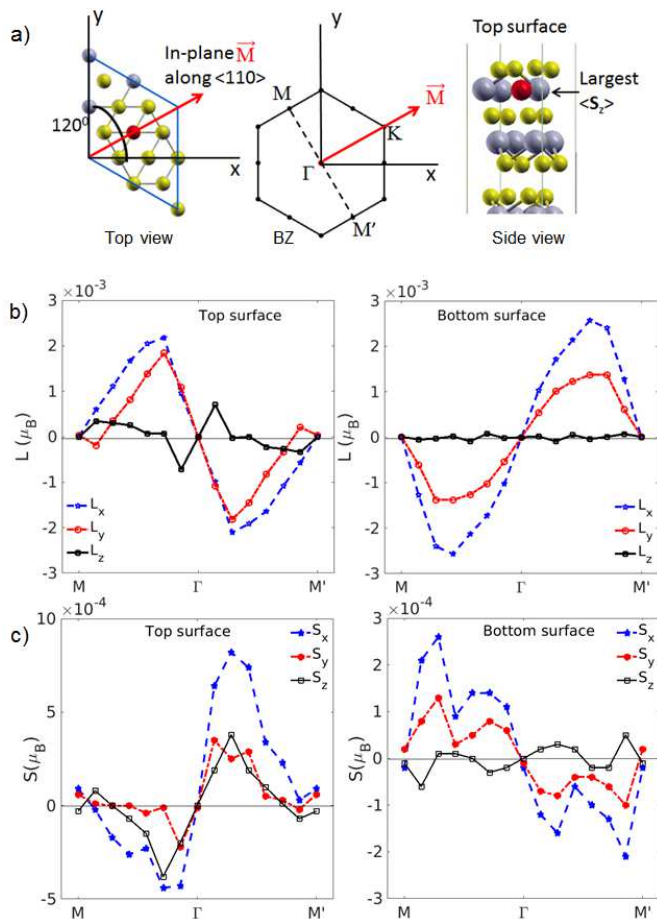


FIG. 2. (a) Top and side view of a Bi_2Se_3 slab, including an impurity atom (red) on the top surface. The direction of the in-plane magnetization relative to the coordinate axes is shown by a red arrow. The BZ shows the M - Γ - M' (dotted line) path along which the expectation values of the operators are calculated. (b) and (c) Expectation values of orbital and spin operators, respectively, for Fe-doped Bi_2Se_3 . At the top surface, expectation values are calculated for the Bi atom that is nearest to the Fe impurity. At the bottom surface a Se atom is used.

$\langle L_z \rangle$, which is most relevant for our purpose, is about an order of magnitude larger at k -points near Γ for the atom at the top surface. Since $\langle L_z \rangle$ is a measure of the strength of the impurity-induced field and the HW effect, we expect its behavior to be reflected on the spin of the surface electrons, as shown in Fig. 2c. Evidently, $\langle S_z \rangle$, which is responsible for opening a gap at the DP, is an order of magnitude larger at the top surface. This result clearly indicates that the impurity-induced field plays a much more dominant role than the HW term in determining a gap at the DP of the topological surface states for an in-plane magnetization.

Based on these DFT results for $S_z^{\text{atom}}(\mathbf{k})$, we can try to make an approximate estimate of the energy gap at the

shifted DP induced by the in-plane impurity potential gradient. According to Fu's theory the energy gap at the DP shifted by an in-plane magnetic field is proportional to $S_z^{\text{atom}}(\mathbf{k}^*)$, where \mathbf{k}^* is the position of the shifted DP. Previous DFT calculations [18] find that for an in-plane magnetization, the gap induced by HW term is < 0.1 meV. Therefore it is not unreasonable to expect that the in-plane potential gradient caused by impurity can give rise to a gap \approx ten times larger, that is, of the order of a few meV, comparable in size to the energy gaps obtained in TIs when the magnetization is out of the plane.

V. CONCLUSIONS

To summarize, based on a continuum model we have predicted that an in-plane electric potential gradient due to surface impurities results in an out-of-plane effective magnetic field, which can contribute to the \mathbf{k} -dependent spin-polarization of the surface electrons of TIs along with Fu's HW effect. Both DFT and TB calculations for Mn- and Fe-doped Bi_2Se_3 thin films fully confirmed this prediction and allowed us to elucidate the mechanism behind this effect. The most significant result of this analysis is that the effect of the impurity-potential-induced field is about one order of magnitude larger than Fu's HW effect (for \mathbf{k} points close to Γ -point) and has significant implications for the gap opening at the DP shifted by the in-plane magnetization. Our DFT calculations show that the normal component of the surface spin-polarization, which is responsible for a gap opening at the DP, is about one order of magnitude larger for those surface electrons that are influenced by impurity potential than those that are just affected by the HW effect. Thus, for an in-plane magnetization, the impurity-potential-induced field can open up a gap at the DP of the same order as the one caused by an out-of-plane magnetization. This important result implies that the QAHE can be realized efficiently in magnetic TIs irrespective of whether magnetization is in-plane or out-of-plane to the surface. Thus our work paves the way for enlarging the domain and enhancing the functionality of magnetic TI materials suitable for observing the QAHE and other topological spin-dependent phenomena. One can envisage exploiting this effect to further control and enhance the magnetic gap at the DP, by engineering doping structures which generate large in-plane gradient and therefore large out-of-plane induced spin-polarizations.

Acknowledgments:- This work was supported by the Swedish Research Council (VR) through Grant No. 621-2014-4785, and by the Carl Tryggers Stiftelse through Grant No. CTS 14:178. Computational resources have been provided by the Lunarc Center for Scientific and Technical Computing at Lund University.

-
- [1] C. L. Kane and E. J. Mele, *Phys. Rev. Lett.* **95**, 146802 (2005).
- [2] M. Z. Hasan and C. L. Kane, *Rev. Mod. Phys.* **82**, 3045 (2010).
- [3] A. Bansil, H. Lin, and T. Das, *Rev. Mod. Phys.* **88**, 021004 (2016).
- [4] X.-L. Qi, R. Li, J. Zang, and S.-C. Zhang, *Science* **323**, 1184 (2009).
- [5] W.-K. Tse and A. H. MacDonald, *Phys. Rev. Lett.* **105**, 057401 (2010).
- [6] I. Garate and M. Franz, *Phys. Rev. Lett.* **104**, 146802 (2010).
- [7] R. Yu, W. Zhang, H.-J. Zhang, S.-C. Zhang, X. Dai, and Z. Fang, *Science* **329**, 61 (2010).
- [8] C.-Z. Chang, J. Zhang, X. Feng, J. Shen, Z. Zhang, M. Guo, K. Li, Y. Ou, P. Wei, L.-L. Wang, Z.-Q. Ji, Y. Feng, S. Ji, X. Chen, J. Jia, X. Dai, Z. Fang, S.-C. Zhang, K. He, Y. Wang, L. Lu, X.-C. Ma, and Q.-K. Xue, *Science* **340**, 167 (2013).
- [9] X. Kou, Y. Fan, M. Lang, P. Upadhyaya, and K. L. Wang, *Solid State Communications* **215216**, 34 (2015).
- [10] C.-Z. K-Chang, W. Zhao, D. Y. Kim, H. Zhang, B. A. Assaf, D. Heiman, S.-C. Zhang, C. Liu, M. H. W. Chan, and J. S. Moodera, *Nat. Mater.* **14**, 473 (2015).
- [11] Y. Ren, J. Zeng, X. Deng, F. Yang, H. Pan, and Z. Qiao, *Phys. Rev. B* **94**, 085411 (2016).
- [12] P. Zhong, Y. Ren, Y. Han, L. Zhang, and Z. Qiao, *Phys. Rev. B* **96**, 241103 (2017).
- [13] Z. Liu, G. Zhao, B. Liu, Z. F. Wang, J. Yang, and F. Liu, *Phys. Rev. Lett.* **121**, 246401 (2018).
- [14] L. Fu, *Phys. Rev. Lett.* **103**, 266801 (2009).
- [15] X. Liu, H.-C. Hsu, and C.-X. Liu, *Phys. Rev. Lett.* **111**, 086802 (2013).
- [16] J. Henk, M. Flieger, I. Maznichenko, I. Mertig, A. Ernst, S. Eremeev, and E. Chulkov, *Phys. Rev. Lett.* **109**, 076801 (2012).
- [17] L. B. Abdalla, L. Seixas, T. M. Schmidt, R. H. Miwa, and A. Fazzio, *Phys. Rev. B* **88**, 045312 (2013).
- [18] F. Hajiheidari, W. Zhang, and R. Mazzarello, *Phys. Rev. B* **94**, 125421 (2016).
- [19] M. F. Islam, C. M. Canali, A. Pertsova, A. Balatsky, S. K. Mahatha, C. Carbone, A. Barla, K. A. Kokh, O. E. Tereshchenko, E. Jiménez, N. B. Brookes, P. Gargiani, M. Valvidares, S. Schatz, T. R. F. Peixoto, H. Bentmann, F. Reinert, J. Jung, T. Bathon, K. Fauth, M. Bode, and P. Sessi, *Phys. Rev. B* **97**, 155429 (2018).
- [20] R. R. Biswas and A. V. Balatsky, *Phys. Rev. B* **81**, 233405 (2010).
- [21] A. M. Black-Schaffer and A. V. Balatsky, *Phys. Rev. B* **85**, 121103 (2012).
- [22] M. R. Mahani, A. Pertsova, M. F. Islam, and C. M. Canali, *Phys. Rev. B* **90**, 195441 (2014).
- [23] Z. Alpichshev, R. R. Biswas, A. V. Balatsky, J. G. Analytis, J.-H. Chu, I. R. Fisher, and A. Kapitulnik, *Phys. Rev. Lett.* **108**, 206402 (2012).
- [24] T. Eelbo, M. Waśniowska, M. Sikora, M. Dobrzański, A. Kozłowski, A. Pulkin, G. Autès, I. Miotkowski, O. V. Yazyev, and R. Wiesendanger, *Phys. Rev. B* **89**, 104424 (2014).
- [25] Y. Xu, J. Chiu, L. Miao, H. He, Z. Alpichshev, A. Kapitulnik, R. R. Biswas, and L. A. Wray, *Nat. Commun.* **8**, 14081 (2017).
- [26] M. Zhong, S. Li, H.-J. Duan, L.-B. Hu, M. Yang, and R.-Q. Wang, *Scientific Reports* **7**, 3971 (2017).
- [27] L. Miao, Y. Xu, W. Zhang, D. Older, S. A. Breitweiser, E. Kotta, H. He, T. Suzuki, J. D. Denlinger, R. R. Biswas, J. G. Checkelsky, W. Wu, and L. A. Wray, *npj Quantum Materials* **3**, 29 (2018).
- [28] P. Sessi, R. R. Biswas, T. Bathon, O. Storz, S. Wilfert, A. Barla, K. A. Kokh, O. E. Tereshchenko, K. Fauth, M. Bode, and A. V. Balatsky, *Nat. Commun.* **7**, 12027 (2016).
- [29] C. R. Ast, J. Henk, A. Ernst, L. Moerschini, M. C. Falub, D. Pacilé, P. Bruno, K. Kern, and M. Gioni, *Phys. Rev. Lett.* **98**, 186807 (2007).
- [30] K. Sakamoto, T. Oda, A. Kimura, K. Miyamoto, M. Tsujikawa, A. Imai, N. Ueno, H. Namatame, M. Taniguchi, P. E. J. Eriksson, and R. I. G. Uhrberg, *Phys. Rev. Lett.* **102**, 096805 (2009).
- [31] M. Kobayashi, I. Muneta, Y. Takeda, Y. Harada, A. Fujimori, J. Krempaský, T. Schmitt, S. Ohya, M. Tanaka, M. Oshima, and V. N. Strocov, *Phys. Rev. B* **89**, 205204 (2014).
- [32] A. Pertsova and C. M. Canali, *New Journal of Physics* **16**, 063022 (2014).
- [33] J. P. Perdew, K. Burke, and M. Ernzerhof, *Phys. Rev. Lett.* **77**, 3865 (1996).
- [34] P. Blaha, K. Schwarz, G. K. H. Madsen, D. Kvasnicka, and J. Luitz, WIEN2K, An Augmented Plane Wave Plus Local Orbitals Program for Calculating Crystal properties (Vienna University of Technology, Austria, 2001).